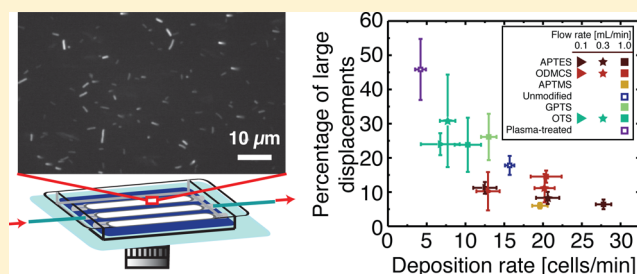


Attachment from Flow of *Escherichia coli* Bacteria onto Silanized Glass SubstratesSumedha Sharma[†] and Jacinta C. Conrad^{*,†,‡}[†]Department of Chemical and Biomolecular Engineering and [‡]Petroleum Engineering Program, University of Houston, Houston, Texas 77006, United States

Supporting Information

ABSTRACT: We investigate the attachment of *Escherichia coli* on silanized glass surfaces during flow through a linear channel at flow rates of 0.1–1 mL/min using confocal microscopy. We assemble layers of organosilanes on glass and track the position and orientation of bacteria deposited on these surfaces during flow with high spatial resolution. We find that a metric based on the degree of the surface-tethered motion of bacteria driven by flagella is inversely correlated with deposition rate, whereas conventional surface characterizations, such as surface energy or water contact angle, are uncorrelated. Furthermore, the likelihood that an initially moving bacterium becomes immobilized increases with increasing deposition rate. Our results suggest that the chemistry and arrangement of silane molecules on the surface influence the transition from transient to irreversible attachment by favoring different mechanisms used by bacteria to attach to surfaces.



INTRODUCTION

Bacteria irreversibly adhere to surfaces in the early stages of formation of bacterial biofilms,¹ which shelter the enclosed bacteria within a protective extracellular polymeric matrix. Biofilms generate significant problems in human health: for example, biofilm-forming bacteria are a major cause of hospital-acquired infections.^{2,3} Similarly, biofouling of a wide variety of industrial and technological surfaces, including oil and water pipelines,⁴ ship hulls,⁵ and food-processing equipment,⁶ generates significant and deleterious costs. The structure and composition of biofilms depend on the interactions between bacteria and surfaces that mediate the initial attachment events.⁷ Designing materials and coatings to prevent the formation of biofilms on surfaces thus requires an understanding of how surface properties affect bacteria–surface interactions.

Physicochemical interactions between bacteria and surfaces are typically described using one of two approaches. In the thermodynamic approach, the change in free energy as bacteria transition from planktonic to surface-attached is described in terms of interfacial tensions between the bacteria, fluid medium, and solid substrate.^{8,9} In the Derjaguin–Landau–Verwey–Overbeek (DLVO) theory applied to bacteria,^{10,11} the free energy is described as a balance between attractive Lifshitz–van der Waals and attractive or repulsive electrostatic forces. Additional forces, such as Lewis acid–base and Brownian forces, are included in the extended DLVO (xDLVO) approach to explain “hydrophobic attractive”¹² and “hydrophilic repulsive”¹³ interactions. Beyond these physicochemical interactions, bacteria may also possess adhesins that enable them to puncture the secondary energy maximum and attach

irreversibly;¹⁴ these include pili,¹⁵ flagella,^{16,17} fimbriae,^{18,19} lipopolysaccharides,²⁰ and extracellular polymeric substances.^{21–23} Adhesins that also serve as motility appendages, such as type IV pili or flagella, directly couple near-surface motility to adhesion.^{24–26} Finally, hydrodynamic forces on the bacterium due to nearby surfaces^{27–29} and the chemistry of the solution^{30–32} modify the physicochemical and/or Brownian interactions and therefore also affect bacterial adhesion.

Surface properties affect the interactions between bacteria and surfaces and thereby modify the extent to which bacteria irreversibly attach to surfaces. For example, surface charge,^{33,34} hydrophobicity/hydrophilicity,^{35–37} and microtopography^{38–40} affect the rate at which bacteria deposit on surfaces. The deposition rate is typically measured by counting the number of bacteria attached to the surface as a function of time.^{19,20} These analyses, however, do not typically characterize the behavior of individual attached bacteria and thus cannot quantify variations in behavior that may generate additional insight into mechanisms of bacterial attachment. A complementary approach is to employ high-throughput bacteria-tracking techniques to analyze the trajectories of hundreds to thousands of individual bacteria on or near surfaces. In this approach, a microscopy movie is translated into a database of searchable trajectories; subsequently, automated searches of these trajectories are designed to identify motility behaviors that are correlated with properties of interest. These techniques have been employed to identify individual and collective

Received: June 12, 2014

Revised: August 22, 2014

Published: August 25, 2014

motility mechanisms used by bacteria on surfaces^{22,24,41–43} and thereby generate a mechanistic understanding of the role of bacterial adhesins during early biofilm formation. By contrast, the role of surface properties in mediating attachment and motility has not been explored through this high-throughput approach. New metrics to characterize the rate of deposition at the scale of individual bacteria will generate an improved understanding of the effects of surface properties on the transition to irreversible attachment.

In this paper, we employ automated high-throughput tracking methods to investigate the transition to irreversible attachment for bacteria deposited during flow onto silanized glass substrates. We use the bacterium *Escherichia coli*, a widely-studied model Gram-negative opportunistic pathogen that is usually benign and easy to isolate and culture in chemical media.⁴⁴ By tracking the position and orientation of every *E. coli* bacterium in microscopy movies acquired as cells are deposited onto surfaces bearing different self-assembled silane layers, we find that the deposition rate over short time scales is poorly correlated with two standard metrics used for surface properties, water contact angle and surface energy. Instead, we develop new metrics to characterize the extent of flagella-driven motion for bacteria that are transiently attached to the surface and show that a high degree of motion is inversely correlated with the rate at which bacteria are deposited. This approach allows us to separately track detaching bacteria and the fate of bacteria that initially exhibit a high degree of surface motion; we find that surfaces with a high deposition rate of bacteria typically have few detaching bacteria and a large fraction of moving bacteria that become immobilized. X-ray photoelectron spectroscopy (XPS) characterization of the silanized glass surfaces suggests that the chemistry and arrangement of silane molecules affect both the initial deposition and the transition to irreversible attachment for a given flow rate. The high-throughput approach described here offers new opportunities to sensitively characterize motility behaviors correlated with this transition across a wide range of surface properties.

MATERIALS AND METHODS

Bacteria Culture. *E. coli* strain MC1061, which is derived from the K12 strain, was used in this study (strain courtesy of Prof. Patrick Cirino and Christopher Frei, University of Houston). A plasmid (pFG10) for an enhanced green fluorescence protein (GFP) and chloramphenicol resistance was introduced into the cells. The plasmid enabled the cells to constitutively express GFP and allowed cells to be visualized under fluorescence without external labeling.

Bacteria were streaked on Luria Bertani agar plates (5 g of yeast extract, 10 g of Bacto tryptone, 5 g of NaCl, 15 g of agar, all from BD Chemicals) containing 25 $\mu\text{g}/\text{mL}$ of chloramphenicol (Spectrum) and incubated overnight at 37 °C (Nuvaire Inc.). Single colonies from the plate were used to inoculate 50 mL of sterile Luria Bertani medium (5 g of yeast extract, 5 g of NaCl, and 10 g of Tryptone per 1 L of medium, BD Chemicals) containing 25 $\mu\text{g}/\text{mL}$ of chloramphenicol and incubated in an orbital incubator shaker (New Brunswick Scientific) at 190 rpm and 37 °C for approximately 17–18 h. To create a dense pellet, cells were centrifuged at 5000g in a Sorvall ST 16 centrifuge (Thermo Fisher Scientific) for 20 min. After pelleting, the cells were resuspended in 0.9% NaCl solution (ionic strength 154 mM). Cells were washed twice in NaCl by repeated mixing, centrifuging, and resuspension to remove the growth medium. Finally, for all imaging experiments the cells were suspended in 154 mM NaCl and diluted volumetrically to an optical density measured at a wavelength of 600 nm (OD_{600}) of 0.42 (with a background subtraction of 0.03 applied), which was measured using a microplate reader (Infinte200 Pro, Tecan). Cells in all experiments were in a stationary

stage of growth, based on a growth curve generated by measuring the OD_{600} of a growing culture at 30 min intervals for 24 h. To approximately correlate the optical density (which measures the biomass concentration) to viable cell number density, a plate count assay was performed. For two different cultures, an optical density of 1 was found to correspond to a viable cell number density of approximately 10^8 colony forming units/mL.

Microbial Adhesion to Hydrocarbons Test (MATH) and Bacterial Electrophoretic Mobility. The percentage hydrophobicity of the cells was measured using the MATH test with two solvents, hexadecane and *n*-dodecane,⁴⁵ as $8.9 \pm 1.3\%$ for *n*-dodecane and $6.9 \pm 3.6\%$ for hexadecane. The electrophoretic mobility of the cells was measured using a NICOMP 380 ZLS ζ -potential analyzer (Particle Sizing Systems) at ionic strengths of 15.4 and 1.54 mM due to working limitations of the instrument. Using the Smoluchowski equation,⁴⁶ we calculated the ζ -potential from the electrophoretic mobility as -42 ± 2 mV at 15.4 mM ionic strength and -58 ± 2 mV at 1.54 mM ionic strength.

Substrate Preparation. Substrates for deposition experiments were prepared by vapor or solution deposition of organosilanes on glass. Prior to deposition, glass coverslips with dimensions 48×65 mm² (thickness 0.13–0.17, Gold Seal) were first cleaned by successive sonication in acetone (Macron, AR grade) and double deionized (DI) water (resistivity 18.2 M Ω cm, Millipore water purification system) and then treated with air plasma for 2 min. For deposition of 3-aminopropyltriethoxysilane (APTES) (99% Sigma) and 3-aminopropyltrimethoxysilane (APTMS) (95%, Gelest), a 1% (wt) solution of silane in ethanol containing 5% DI water was prepared and stirred for 5 min. Clean slides were immersed in the solution for 5 min with continuous stirring. Slides were rinsed in ethanol (200 proof, Devcon) and 2-propanol (99%, Sigma); APTMS-coated slides were additionally rinsed with DI water. Slides were dried under nitrogen stream and baked at 110 °C for 10 min. To deposit glycidoxypropyltriethoxysilane (GPTS) (95%, Gelest), clean slides were immersed in a 0.02 M GPTS solution in toluene (98% Sigma) for 210 min. After immersion, slides were rinsed twice in each of toluene, methanol (98%, Devcon), and DI water and dried under nitrogen. Octyldimethylchlorosilane (ODMCS) (95% Gelest) was deposited from vapor in a vacuum desiccator held at 30 mmHg for 30 h. After deposition of ODMCS, the slides were sonicated in four solutions—a 1:1 (v/v) mixture of deionized water and chloroform for 5 min, toluene for 2 min, isopropyl alcohol for 1 min, and finally deionized water for 1 min—and dried under nitrogen. Octadecyltrichlorosilane (OTS) (95%, Gelest) was deposited by immersing a clean slide in a freshly prepared 0.5 mM OTS solution in anhydrous toluene (99.8%, Sigma) for 17 h in an airtight jar. After deposition, the slides were sonicated in chloroform (99.8%, Sigma), acetone (HPLC grade) and DI water sequentially and dried in nitrogen. All silanized substrates were placed in petri dishes, sealed with Parafilm, and stored in a desiccator for no more than 2 days before use.

Surface Characterization. Water contact angles were measured using a Dataphysics OCA 15EC goniometer. Reported data correspond to at least five spot measurements made on three surfaces. Contact angles for two other test liquids, ethylene glycol (99%, Alfa Aesar) and diiodomethane (99%, Alfa Aesar), were measured for each surface, and the surface energy was calculated using algorithms built into the instrument's analysis package, which were based on the method of Wu.⁴⁷ To characterize the elemental composition of APTES- and APTMS-coated surfaces, photoelectrons produced via a monochromatic Al K α X-ray source (1486.6 eV) operated at 350 W were collected on a Physical Electronics model 5700 X-ray photoelectron spectroscopy (XPS) instrument. The analyzed area, collection solid cone, and takeoff angle were set at 800 μm , 5°, and 45°, respectively. An applied pass energy of 23.52 eV resulted in an energy resolution of better than 0.51 eV. All spectra were acquired after vacuum of 5×10^{-9} Torr was attained. The binding energy scales were referenced to 284.6 eV, corresponding to the maximum intensity for a C 1s spectrum. Data processing was carried out using the Multipak software package (Ulvac-PHI, Physical Electronics). A Shirley background subtraction routine⁴⁸ was applied throughout.

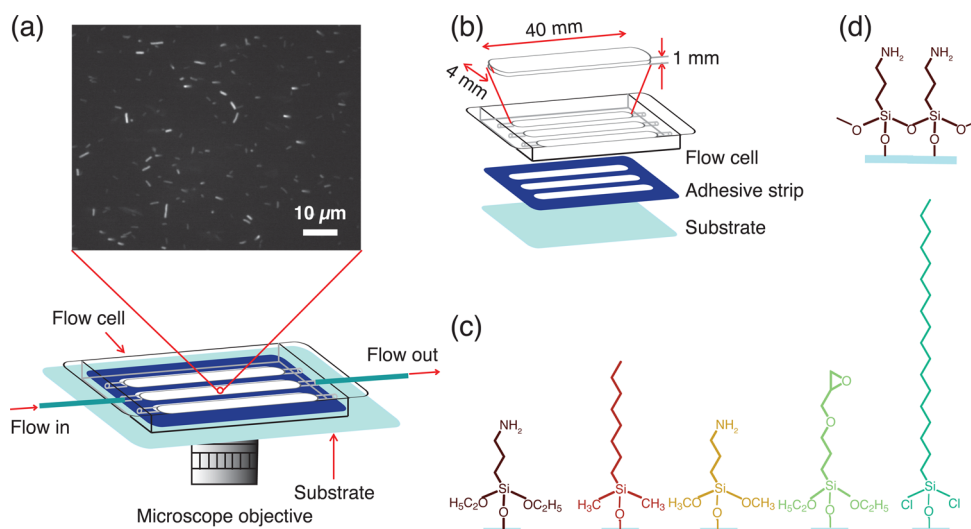


Figure 1. (a) Schematic of the experimental setup used in flow cell experiments. (b) Exploded view of flow cell assembly. (c) Chemical structures of single organosilane molecules as expected to be deposited on glass substrates, left to right: 3-aminopropyltriethoxysilane (APTES), octyldimethylchlorosilane (ODMCS), 3-aminopropyltrimethoxysilane (APTMS), 3-glycidoxypropyltriethoxysilane (GPTS), and octadecyltrichlorosilane (OTS). (d) Structure of an APTES monolayer attached to glass, showing expected cross-linked structure.

The ζ -potentials of silane-coated nanoparticles of diameter of 170 nm were measured using a NanoBrook ZetaPALs (Brookhaven Instruments) analyzer at an ionic strength of 154 mM (see the Supporting Information for additional details).

Flow Experiments and Image Analysis. In deposition experiments, suspensions of bacteria were flowed through a linear channel⁴⁹ (Figure 1a) at volumetric flow rates of $Q = 0.1, 0.3,$ or 1 mL/min using a syringe pump (model 11, Harvard Apparatus). The experimental setup (Figure 1a) consisted of a coverglass substrate (silane-functionalized or bare/plasma treated, as a control) onto which a molded polyethylene cell (Biocentrum DTU) was attached with double-sided adhesive tape (Dow Corning Electronics). The width, height, and length of the flow channel were $W = 4$ mm, $2b = 2$ mm, and $h = 40$ mm, respectively (Figure 1b). At flow rates of $0.1, 0.3,$ and 1 mL/min, the shear rates were $\dot{\gamma} = 3Q/2Wb^2 = 0.625, 1.875,$ and 6.25 s^{-1} , respectively, and the shear stresses were $\sigma = 3Q\mu/2Wb^2 = 0.56, 1.66,$ and 5.56 mN/m^2 , respectively, where $\mu = 0.89$ mPa·s was the viscosity of water. Bacteria deposited on the substrates during flow were imaged using a confocal fluorescence scanner (VT Infinity, Visitech) attached to a Leica DM4000 inverted microscope equipped with a $100\times$ oil immersion lens (HCX PL APO of numerical aperture 1.4) and laser excitation source ($\lambda = 488$ nm). One image with an exposure time of 0.3 s and a pixel size of 0.125 ± 0.0006 μm was acquired every 3 s using an ORCA 200 camera (Hamamatsu) that was controlled by Voxcell Scan software (Visitech). In a typical deposition experiment, 210 images with an area of 84×64 μm^2 (corresponding to 672 pixels \times 512 pixels) were acquired after at least two bacteria were deposited in the field of view. Experiments on each surface were performed in triplicate; at least one experiment in each trio was performed on a different substrate and with a different bacteria culture.

Single bacterium-tracking algorithms, written in IDL (Exelis VIS) and based on algorithms used to track rodlike colloidal particles⁵⁰ and modified for elongated bacteria,⁴¹ were employed to locate and track every bacterium in a time series of microscopy images. Further analysis of the attachment and detachment rates and orientations of bacteria was performed using routines written in Matlab (MathWorks) and in IDL.

RESULTS AND DISCUSSION

Earlier experiments on *E. coli* showed that self-assembled layers of silanes can inhibit bacterial adhesion and biofilm formation^{51,52} and that the chemical details of the silane layer sensitively affected the force of bacterial adhesion.⁵³ We

therefore deposited silanes on glass surfaces as a model system in which to investigate the transition to irreversible attachment across a range of surface chemistries. We first measured the number of *E. coli* bacteria that attached to each surface over time when exposed to a constant flow rate of 1 mL/min. The number of cells deposited on the surface over time varied with the surface chemistry, as shown in Figure 2. At times greater

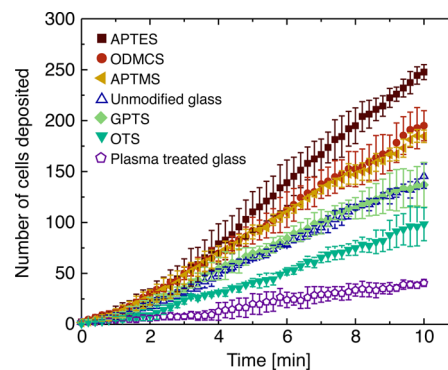


Figure 2. Number of *E. coli* bacteria deposited on the surface as a function of time for surfaces bearing silane molecules (closed symbols) and for glass surfaces without silanes (open symbols) at a suspension flow rate of 1 mL/min. The initial time for each experiment ($t = 0$) was chosen as the time at which two cells were initially deposited on the surface. Error bars indicate standard deviations over three replicates.

than 2 min, the slope of each curve was nearly linear, allowing the rate at which bacteria were deposited on each surface to be calculated from the long-time slope.

The deposition rate of *E. coli* at a flow rate of 1 mL/min was a nonmonotonic function of two surface properties frequently used to characterize surfaces, surface hydrophobicity (measured as water contact angle) and surface energy (Figure 3). The greatest deposition rates were observed for hydrophilic APTES and APTMS surfaces and hydrophobic ODMCS surfaces, whereas the lowest deposition rates were observed on the extremely hydrophilic plasma-treated glass surface and on the

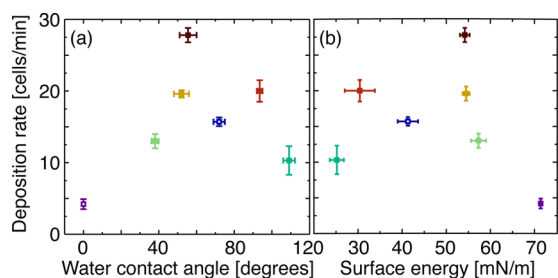


Figure 3. Deposition rate (cells/min) at a suspension flow rate of 1 mL/min as a function of (a) the water contact angle and (b) the surface energy. Error bars indicate standard deviations measured from triplicate replicates (for deposition rate), at least five spot measurements on at least three substrates (for water contact angle), and at least two surfaces (for surface energy). Colors correspond to those used in Figure 2

superhydrophobic OTS surface. Moreover, surfaces of similar energy could exhibit strikingly different rates of bacterial deposition. The cationic APTES and APTMS surfaces and the neutrally charged GPTS surface had similar surface energies. The deposition rate on GPTS, however, was comparable to that on unmodified clean glass, whereas the rate on the two cationic surfaces was a factor of 2 greater. Measurements of the ζ -potential of silane-functionalized nanoparticles of diameter 170 nm showed a greater correlation to deposition rate (Supporting Information, Figure S1), although surfaces of similar ζ -potential (e.g., approximately neutral GPTS, ODMCS, and OTS or positively-charged APTES and APTMS) still exhibited differences in deposition rate. These results indicated that surface chemistry affected the rate at which cells were initially deposited in a nontrivial fashion, consistent with earlier reports that argued that molecular details sensitively affected the extent of deposition.⁵³

To gain insight into the mechanisms that mediated initial attachment of *E. coli*, we examined the trajectories of every bacterium deposited onto these surfaces. Although most bacteria (~90%) remained in the field of view for at least 24 s and were thus at least transiently attached to the surface, the degree of motion varied significantly between trajectories. Some bacteria were nearly immobile after attaching to the surface (Figure 4a), whereas other bacteria flipped back and forth between two positions (Figure 4b) or rotated in a circle while tethered (Figure 4c). *E. coli* possesses only one type of appendage that generates rotation, the flagellum, and flagellum-tethered *E. coli* can rotate when attached to surfaces;^{54–56} we therefore posit the observed flipping and rotating was generated by flagella. This transient motion, which did not generate net

displacement, is different from other transient mechanisms used by *E. coli* to attach to surfaces, such as weak rolling adhesion mediated by fimbriae,⁵⁷ in which the center-of-mass of the cell translates laterally. From the microscopy movies, we observed that bacteria were more likely to flip and rotate on surfaces with lower deposition rates (e.g., OTS, Movie S1, and plasma-treated glass, Movie S2, Supporting Information) than on surfaces to which they rapidly attached (e.g., APTES, Movie S3, Supporting Information).

To quantify differences in the extent of transient motion of bacteria on surfaces of varying chemistry, we calculated the displacement of the centroid of each bacterium at each time step. The displacements of the bacteria shown in Figure 4a–c increased from top to bottom, consistent with an increase in the extent of motion that is likely driven by transient flagella-mediated attachment. We therefore calculated a cumulative percentage of displacements that were smaller than a cutoff value D , measured in micrometers. At every fixed value of D , the APTES-coated and plasma-treated glass surfaces exhibited the highest and lowest cumulative percentages of displacements that were smaller than D , respectively (Figure 5). Many

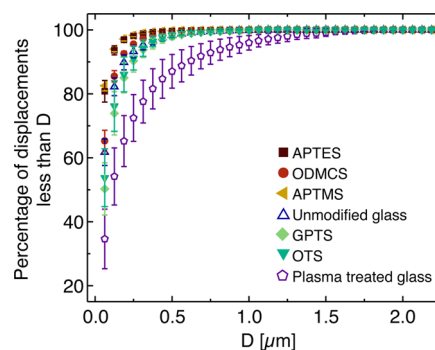


Figure 5. Cumulative percentage of bacteria deposited at a suspension flow rate of 1 mL/min that exhibit a displacement of less than D micrometers for surfaces of different chemistries. Error bars indicate the standard deviation over three replicates. Symbols and colors correspond to those used in Figure 2. The total number of attached cell positions analyzed for each replicate on each substrate was as follows: APTES ($N = 22\,251, 22\,337, 26\,987$), ODMCS ($N = 17\,782, 20\,673, 21\,182$), APTMS ($N = 18\,863, 19\,344, 19\,533$), unmodified glass ($N = 12\,228, 13\,943, 14\,252$), GPTS ($N = 11\,563, 13\,753, 13\,995$), OTS ($N = 8399, 9826, 10\,229$), and plasma-treated glass ($N = 3483, 4358, 4715$).

antimicrobial peptides bear positively charged moieties, and positively charged surfaces can exhibit antimicrobial activity.⁵⁸ We thus performed a live–dead assay to determine whether the

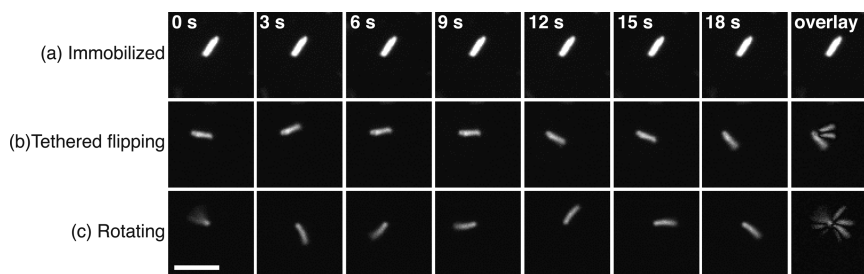


Figure 4. Time series of confocal micrographs depicting three characteristic types of bacterial motion: (a) immobilized; (b) tethered flipping, in which the bacterium flips between few positions in the surface plane; and (c) rotating while tethered to the surface. The last image in each row is an overlay of all images in the time series. The initial time step (0 s) is different for each series. The scale bar is 5 μm .

APTES and APTMS surfaces were bactericidal. Staining of deposited cells with propidium iodide showed that over 90% of cells deposited onto APTES and APTMS remained viable, and the proportion of dead cells observed on the cationic surfaces (APTES, APTMS) did not significantly differ from that on unmodified glass substrates (Table S1, Supporting Information). Finally, at every fixed value of D , bacteria attached to neutral GPTS surfaces exhibited significantly more motion than those attached to cationic APTES or APTMS surfaces, suggesting that different mechanisms mediate deposition on surfaces of different chemistries yet similar surface energies.

This interpretation of the cumulative percentage displacements in Figure 5 suggests that the degree of surface motion may signal the propensity of bacteria to attach to these surfaces. We defined as a motility metric the percentage of displacements greater than 0.12 micrometers, corresponding to the second bin in Figure 5. For a suspension flow rate of 1 mL/min, this metric was inversely correlated with the deposition rate ($R^2 = 0.84$), as shown in Figure 6: surfaces with a large (small) fraction of

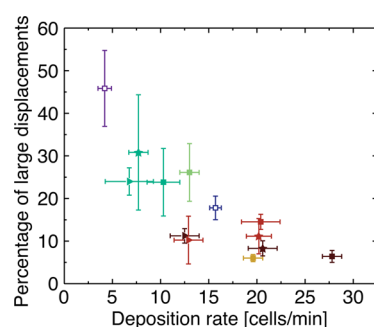


Figure 6. Percentage of large displacements (greater than 0.12 μm) as a function of deposition rate (in cells/min). Error bars indicate the standard deviation over three replicates. Colors correspond to those used in Figure 2. Shapes correspond to measurements at different suspension flow rates for selected substrates: 0.1 mL/min (triangles), 0.3 mL/min (stars), and 1.0 mL/min (squares). The total number of attached cell positions analyzed for each replicate acquired at 1.0 mL/min on each substrate was as follows: APTES ($N = 22\,251, 22\,337, 26\,987$), ODMCS ($N = 17\,782, 20\,673, 21\,182$), APTMS ($N = 18\,863, 19\,344, 19\,533$), unmodified glass ($N = 12\,228, 13\,943, 14\,252$), GPTS ($N = 11\,563, 13\,753, 13\,995$), OTS ($N = 8399, 9826, 10\,229$), and plasma-treated glass ($N = 3483, 4358, 4715$).

moving bacteria exhibited low (high) deposition rates. Differences between the percentages of displacements greater than 0.12 micrometers between any two pairs of substrates were significant at the level of $p < 0.01$ (see Table S2, Supporting Information). This inverse correlation is striking when compared to the lack of correlation seen between deposition rate and the traditional surface characterization metrics shown in Figures 3 and S1 (Supporting Information) ($R^2 = 0.11$ for water contact angle, $R^2 = 0.039$ for surface energy, and $R^2 = 0.193$ for ζ -potential). A similar correlation was obtained for other cutoff values for the cumulative displacement. Because the mechanisms of surface motion (flipping and rotation, as in Figure 4) were driven by flagella, these results suggest that attachment mediated by a flagellum is weaker than that mediated by strong and short-ranged electrostatic, van der Waals, and/or hydrophobic interactions between the bacterial body and the surface.

Experiments performed at lower flow rates (0.1 and 0.3 mL/min) also exhibited the same trend of increasing deposition rate

with decreasing motility within experimental errors ($R^2 = 0.67$), as shown by the triangles and stars in Figure 6. By contrast, surface energy, water contact angle, and ζ -potential could not account for changes in deposition rate as a function of flow rate. Furthermore, extended DLVO (xDLVO) calculations showed that the silanized surface with the highest and lowest deposition rates at 1 mL/min, APTES and OTS, respectively, both exhibited a deep primary minimum (Figure S2, Supporting Information), suggesting that both surfaces would favor strong adhesion. Our motility metric may therefore provide information on time-dependent and/or dynamic bacterial adhesion that cannot be obtained via other methods to characterize surfaces.

We further probed the relationship between the degree of surface motion and the deposition rate by classifying the motion and attachment fate of each transiently attached bacterium. Trajectories of bacteria of duration shorter than 24 s, corresponding to bacteria that attach to the surface for only a short time, are indicated by gray bars in Figure 7. The

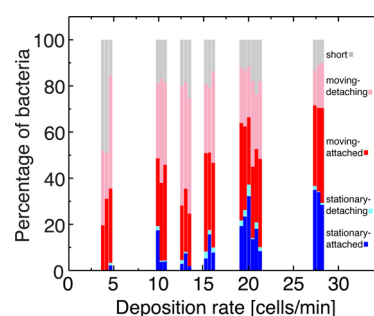


Figure 7. Classification of bacteria as a function of deposition rate, as stationary or moving and as attached or detaching, for a suspension flow rate of 1 mL/min. Colors: stationary and attached (dark blue), stationary and detaching (light blue), moving and attached (dark red), moving and detaching (light red); bacteria with trajectories too short to be analyzed are shown in gray. Each vertical bar represents one replicate experiment at a given deposition rate. The total number of bacteria analyzed for each replicate on each substrate was as follows: APTES ($N = 315, 345, 352$), ODMCS ($N = 321, 405, 435$), APTMS ($N = 244, 282, 298$), unmodified glass ($N = 230, 262, 270$), GPTS ($N = 296, 309, 316$), OTS ($N = 187, 205, 218$), and plasma-treated glass ($N = 90, 106, 158$).

percentage of bacteria that exhibited such short trajectories was inversely proportional to the deposition rate, with the smallest percentage of short trajectories observed on APTES and APTMS surfaces and the largest percentage observed on plasma-treated glass. Longer trajectories in which the centroid of the bacterium was displaced by at least 0.12 micrometers between consecutive images were classified as moving; all other longer trajectories were classified as stationary. Longer trajectories of bacteria that left the field of view before the end of the experiment were classified as detaching; all other longer trajectories were classified as attached. For all surfaces, only a tiny fraction of stationary bacteria detached during the experiment. Generally, as the deposition rate increased, the percentage of stationary and attached trajectories increased and the percentage of moving and detaching trajectories decreased; this metric was less sensitive, however, to the initial flow rate than to the surface chemistry (Figure S4, Supporting Information). The number of bacteria that detached during each experiment at a suspension flow rate of 1 mL/min typically decreased slightly as the deposition rate increased, as

shown in Figure 8; this trend, however, did not hold at lower flow rates, where the detachment rates were uniformly lower

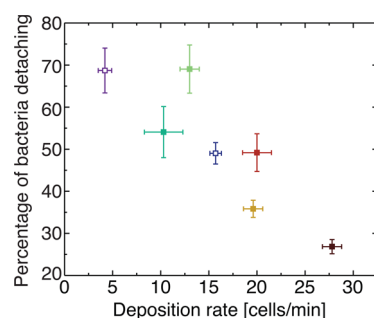


Figure 8. Percentage of bacteria that detach during each experiment as a function of deposition rate for a suspension flow rate of 1 mL/min. Error bars indicate standard deviation over three replicates. Colors correspond to those used in Figure 2. The total number of detaching bacteria analyzed for each replicate on each substrate was as follows: APTES ($N = 315, 345, 352$), ODMCS ($N = 321, 405, 435$), APTMS ($N = 244, 282, 298$), unmodified glass ($N = 230, 262, 270$), GPTS ($N = 296, 309, 316$), OTS ($N = 187, 205, 218$), and plasma-treated glass ($N = 90, 106, 158$).

(Figure S5, Supporting Information). Finally, surfaces on which a large fraction of bacteria exhibited a high degree of surface motion through flagellum-driven flipping or rotation exhibited reduced deposition rates. This observation is consistent with either or both of two potential explanations: flagellum-driven motion helps cells to detach²⁴ or that the surface properties correlated with high deposition rates increase the likelihood that bacteria attach irreversibly using other mechanisms.

To attempt to distinguish between these explanations, we classified the attachment fate of bacteria that initially exhibited a large degree of motion and were presumably initially attached via the flagellum. We first subdivided each trajectory of length greater than 24 s into equal thirds. Bacteria whose centroids underwent a large displacement (of greater than 0.12 micrometers) in the first third of their surface dwell time were classified as initially moving. We subsequently determined the fate of each initially moving bacterium by searching its trajectory for large displacements in the remaining thirds. Trajectories that exhibited at least one large centroid displacement in each third were classified as moving; trajectories in which no large centroid displacements were seen in the last third were classified as converted to stationary (Figure S6, Supporting Information). All other behavior was classified as intermediate. The percentage of initially moving bacteria whose fate is moving, stationary, or intermediate is shown as a function of deposition rate in Figure 9: increased deposition rate was correlated with an increase in the percentage of bacteria that converted from moving to stationary over the duration of our experiments. Bacteria most readily became immobilized on the two cationic surfaces (APTES and APTMS) but remained motile on surfaces that resisted initial attachment (plasma-treated glass and OTS). Conversion to immobility depended less on flow rate than on surface chemistry (Figure S7, Supporting Information). This result suggests that the fate of bacteria initially attached by the flagellum depends on the surface properties, with strong and short-ranged electrostatic interactions succeeding the apparently weaker initial attachment frequently mediated by flagella. This mechanism is complementary to the proposed role of

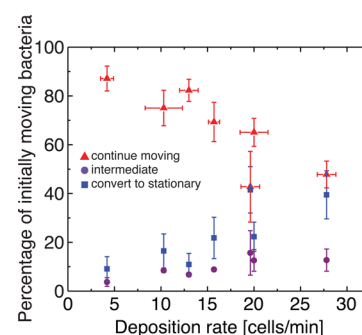


Figure 9. Percentage of initially moving bacteria that continue moving (red triangles), convert to stationary (blue squares), and exhibit an intermediate behavior (purple circles). Error bars indicate standard deviation over three replicates acquired at a suspension flow rate of 1 mL/min. The total number of initially moving bacteria analyzed for each replicate on each substrate was as follows: APTES ($N = 108, 129, 138$), ODMCS ($N = 145, 224, 243$), APTMS ($N = 106, 111, 124$), unmodified glass ($N = 133, 139, 176$), GPTS ($N = 182, 206, 206$), OTS ($N = 102, 132, 133$), and plasma-treated glass ($N = 52, 68, 80$).

flagella in adhesion at low ionic strengths, in which flagella allow bacteria to pierce an unfavorable energetic barrier near the surface.¹⁴

Our results indicate that the rate of deposition and the attachment fate of bacteria on surfaces depend on the surface chemistry. We found significantly less deposition on the OTS surface than on the ODMCS surface, although both surfaces were hydrophobic. OTS has a longer alkyl chain (18 carbons) than ODMCS (8 carbons); ellipsometry measurements on OTS and ODMCS layers on silicon substrates indicated that OTS formed a thicker layer (3.5 ± 0.3 nm) than ODMCS (1.43 ± 0.09 nm) (Table S4, Supporting Information). We therefore posit that the longer OTS chain somewhat hindered bacteria from accessing the energetic minimum very close to the surface. Our results are consistent with earlier reports of reduced deposition of *E. coli* on OTS.^{29,53}

More surprisingly, we observed significantly different deposition rates on the cationic APTES and APTMS, which both bear aminopropyl functional groups and exhibit chemical differences only in the length of the side chains. To gain insight into the molecular-scale origins of the differences in deposition rates, we used XPS and ellipsometry to characterize the properties of these two surfaces (Supporting Information, section S5). First, we used XPS to determine the elemental composition of the silane layer. The presence of a nitrogen (N 1s) peak on both surfaces confirmed the successful deposition of the silanes. Assuming monolayer deposition, the surface densities of the two molecules were nearly equal (4.3 molecules/nm² for APTES and 4.8 molecules/nm² for APTMS). The ratio of C:N on APTES (7:1) was greater than that for APTMS (4:1); if the silane layer were completely cured, then the C:N ratio should be 3:1 for each monolayer. The variation from the ideal C:N ratio suggested that APTMS layers were more cross-linked than APTES layers, which may affect the orientation of the molecules.⁵⁹ Second, we replicated our deposition protocol to create silane layers on silicon wafers and directly measured the layer thickness using spectrophotometric ellipsometry (Supporting Information, Table S4). The thicknesses of the APTES and APTMS layers on the silicon wafers were 1.7 ± 0.3 and 2.46 ± 0.04 nm, respectively, consistent with an APTMS multilayer. These measurements suggest that the differences in the deposition rate may arise

from differences in the arrangement (structure, orientation, and layer thickness) of the silane molecules.

CONCLUSIONS

We investigated the transition from transient to irreversible attachment of *E. coli* bacteria deposited onto surfaces coated with self-assembled silanes. By analyzing the trajectories of hundreds of bacteria on each surface, we found that the rate at which bacteria were deposited varied nonmonotonically with surface wettability and energy. Instead, we found that deposition rate was inversely correlated with the degree of surface-attached flagella-driven motion. For a given flow rate, bacteria less readily detached and more readily became immobilized on the surfaces onto which they most rapidly deposited. We posit that flagella enable bacteria to transiently attach to surfaces; the fate of transiently attached bacteria, however, is ultimately determined by physicochemical interactions (electrostatic or van der Waals) between bacteria and surfaces. Because the transition from transient to immobilized attachment was also correlated with short-time deposition rate, our results suggest that initial transient surface motility may serve as a metric to rapidly determine the efficacy of surfaces to reduce fouling by bacteria and thereby speed the design of improved antifouling materials for medical, technological, and environmental settings.

These initial results suggest multiple pathways for future studies. First, we examined only the initial rate of deposition of bacteria over relatively short times; as bacteria continue to attach over long time scales, we expect that that interactions between bacteria may influence the deposition rate and the transition to irreversible attachment (as suggested by Figure 9). Experiments to correlate initial motion to long-time deposition are required to establish the predictive power of the correlations that we identify here. Second, we showed that our motility metric inversely correlates with deposition rate across multiple flow rates. Variations in detachment rates, however, suggest that bacteria may use different shear-rate-dependent attachment mechanisms on surfaces of different properties; this idea is consistent with earlier experiments on *E. coli* that suggest that the role of flagella in initial attachment changes as the flow rate is increased.⁶⁰ Future experiments using motility- and appendage- or adhesin-deficient mutants will provide further insight into the roles of motility on initial attachment. Finally, we examined only one strain of *E. coli*. Bacteria that readily form biofilms, such as the opportunistic Gram-negative pathogen *Pseudomonas aeruginosa*, release extracellular polymeric substances (EPS) that modify the surface properties and facilitate initial adhesion and attachment⁶¹ and microcolony formation.²² Experiments in biofilm-forming strains may therefore provide insight into the role of EPS in the transition from transient to irreversible attachment. We expect that applying our high-throughput methods to analyze bacterial trajectories in these different scenarios will provide additional insight into the role of bacterial, surface, and fluid conditions on the transition to irreversible adhesion.

ASSOCIATED CONTENT

Supporting Information

Movies of bacterial deposition, ζ -potential measurements, live-dead cell assay, extended DLVO calculations, additional motility metrics and measurements, XPS and ellipsometry results and discussion, and cell number table. This material is available free of charge via the Internet at <http://pubs.acs.org>.

AUTHOR INFORMATION

Corresponding Author

*E-mail: jconrad@uh.edu.

Notes

The authors declare no competing financial interests.

ACKNOWLEDGMENTS

We acknowledge support from the National Science Foundation (DMR-1151133). This work was also supported in part by National Science Foundation Grant No. PHYS-1066293 and the hospitality of the Aspen Center for Physics. We thank Prof. Patrick Cirino and Christopher Frei, for the *E. coli* strain; Prof. Richard Willson and Dr. Uli Strych, for access to bacteria culture equipment; Prof. Gila Stein, for access to ellipsometry and goniometry instruments; Indranil Mitra, for silanization equipment and assistance; Prof. Vincent Donnelly, Shyam Sridhar, and Dr. Boris Makarenko, for XPS measurements; Prof. Vincent Donnelly and Dr. Jack Jacob, for valuable discussions regarding XPS analysis; and Prof. Michael Wong and Varun Shenoy, for use of their ζ -potential instrument.

REFERENCES

- Hall-Stoodley, L.; Costerton, J. W.; Stoodley, P. Bacterial biofilms: From the natural environment to infectious diseases. *Nat. Rev. Microbiol.* **2004**, *2* (2), 95–108.
- Costerton, J. W.; Stewart, P. S.; Greenberg, E. P. Bacterial biofilms: A common cause of persistent infections. *Science* **1999**, *284* (5418), 1318–1322.
- Donlan, R. Biofilms and device-associated infections. *Emerg. Infect. Dis.* **2001**, *7* (2), 277–281.
- Li, K.; Whitfield, M.; Van Vliet, K. J. Beating the bugs: Roles of microbial biofilms in corrosion. *Corros. Rev.* **2013**, *31* (3–6), 73–84.
- Schultz, M.; Swain, G. The influence of biofilms on skin friction drag. *Biofouling* **2000**, *15* (1–3), 129–139.
- Verran, J.; Airey, P.; Packer, A.; Whitehead, K. A. Microbial retention on open food contact surfaces and implications for food contamination. *Adv. Appl. Microbiol.* **2008**, *64*, 223–246.
- Busscher, H. J.; van der Mei, H. C. Physico-chemical interactions in initial microbial adhesion and relevance for biofilm formation. *Adv. Dent. Res.* **1997**, *11* (1), 24–32.
- Absolom, D. R.; Lamberti, F. V.; Policova, Z.; Zingg, W.; van Oss, C. J.; Neumann, A. W. Surface thermodynamics of bacterial adhesion. *Appl. Environ. Microbiol.* **1983**, *46* (1), 90–97.
- Busscher, H. J.; Weerkamp, A. H.; van der Mei, H. C.; van Pelt, A. W. J.; de Jong, H. P.; Arends, J. Measurement of the surface free energy of bacterial cell surfaces and its relevance for adhesion. *Appl. Environ. Microbiol.* **1984**, *48* (5), 980–983.
- Marshall, K. C.; Stout, R.; Mitchell, R. Mechanism of the initial events in the sorption of marine bacteria to surfaces. *Journal of General Microbiology* **1971**, *68* (3), 337–348.
- van Loosdrecht, M. C. M.; Lyklema, J.; Norde, W.; Zehnder, A. J. B. Bacterial adhesion—A physicochemical approach. *Microb. Ecol.* **1989**, *17* (1), 1–15.
- Wood, J.; Sharma, R. How long is the long-range hydrophobic attraction? *Langmuir* **1995**, *11* (12), 4797–4802.
- Elimelech, M. Indirect evidence for hydration forces in the deposition of polystyrene latex colloids on glass surfaces. *J. Chem. Soc. Faraday Trans.* **1990**, *86* (9), 1623.
- Hori, K.; Matsumoto, S. Bacterial adhesion: From mechanism to control. *Biochem. Eng. J.* **2010**, *48* (3), 424–434.
- Burrows, L. L. *Pseudomonas aeruginosa* twitching motility: Type IV pili in action. *Annu. Rev. Microbiol.* **2012**, *66* (1), 493–520.
- Diaz, C.; Schilardi, P. L.; Salvarezza, R. C.; Fernandez Lorenzo de Mele, M. A. Have flagella a preferred orientation during early stages of biofilm formation? AFM study using patterned substrates. *Colloids Surf., B* **2011**, *82* (2), 536–542.

- (17) Friedlander, R. S.; Vlamakis, H.; Kim, P.; Khan, M.; Kolter, R.; Aizenberg, J. Bacterial flagella explore microscale hummocks and hollows to increase adhesion. *Proc. Natl. Acad. Sci. U. S. A.* **2013**, *110* (14), 5624–5629.
- (18) Forero, M.; Thomas, W.; Bland, C.; Nilsson, L. M.; Sokurenko, E. V.; Vogel, V. A catch-bond based nanoadhesive sensitive to shear stress. *Nano Lett.* **2004**, *4* (9), 1593–1597.
- (19) Rodrigues, D. F.; Elimelech, M. Role of type 1 fimbriae and mannose in the development of *Escherichia coli* K12 biofilm: From initial cell adhesion to biofilm formation. *Biofouling* **2009**, *25* (5), 401–411.
- (20) Walker, S. L.; Redman, J. A.; Elimelech, M. Role of cell surface lipopolysaccharides in *Escherichia coli* K12 adhesion and transport. *Langmuir* **2004**, *20* (18), 7736–7746.
- (21) Kim, H. N.; Hong, Y.; Lee, I.; Bradford, S. A.; Walker, S. L. Surface characteristics and adhesion behavior of *Escherichia coli* O157:H7: Role of extracellular macromolecules. *Biomacromolecules* **2009**, *10* (9), 2556–2564.
- (22) Zhao, K.; Tseng, B. S.; Beckerman, B.; Jin, F.; Gibiansky, M. L.; Harrison, J. J.; Luijten, E.; Parsek, M. R.; Wong, G. C. L. Psl trails guide exploration and microcolony formation in *Pseudomonas aeruginosa* biofilms. *Nature* **2013**, *497* (7449), 388–391.
- (23) Cooley, B. J.; Thatcher, T. W.; Hashmi, S. M.; L'Her, G.; Le, H. H.; Hurwitz, D. A.; Provenzano, D.; Touhami, A.; Gordon, V. D. The extracellular polysaccharide Pel makes the attachment of *P. aeruginosa* to surfaces symmetric and short-ranged. *Soft Matter* **2013**, *9* (14), 3871–3876.
- (24) Conrad, J. C.; Gibiansky, M. L.; Jin, F.; Gordon, V. D.; Motto, D. A.; Mathewson, M. A.; Stopka, W. G.; Zelasko, D. C.; Shrout, J. D.; Wong, G. C. L. Flagella and pili-mediated near-surface single-cell motility mechanisms in *P. aeruginosa*. *Biophys. J.* **2011**, *100* (7), 1608–1616.
- (25) Conrad, J. C. Physics of bacterial near-surface motility using flagella and type IV pili: Implications for biofilm formation. *Res. Microbiol.* **2012**, *163*, 619–629.
- (26) Maier, B. The bacterial type IV pilus system—A tunable molecular motor. *Soft Matter* **2013**, *9* (24), 5667–5671.
- (27) Lauga, E.; DiLuzio, W. R.; Whitesides, G. M.; Stone, H. A. Swimming in circles: Motion of bacteria near solid boundaries. *Biophys. J.* **2006**, *90* (2), 400–412.
- (28) Hill, J.; Kalkanci, O.; Mcmurry, J. L.; Koser, H. Hydrodynamic surface interactions enable *Escherichia coli* to seek efficient routes to swim upstream. *Phys. Rev. Lett.* **2007**, *98* (6), 068101.
- (29) Wang, H.; Sodagari, M.; Ju, L.-K.; Newby, B.-m. Z. Effects of shear on initial bacterial attachment in slow flowing systems. *Colloids Surf., B* **2013**, *109*, 32–39.
- (30) Vigeant, M. A.-S.; Ford, R. M. Interactions between motile *Escherichia coli* and glass in media with various ionic strengths, as observed with a three-dimensional-tracking microscope. *Appl. Environ. Microbiol.* **1997**, *63* (9), 3474–3479.
- (31) Olsson, A. L. J.; Arun, N.; Kanger, J. S.; Busscher, H. J.; Ivanov, I. E.; Camesano, T. A.; Chen, Y.; Johannsmann, D.; Van Der Mei, H. C.; Sharma, P. K. The influence of ionic strength on the adhesive bond stiffness of oral streptococci possessing different surface appendages as probed using AFM and QCM-D. *Soft Matter* **2012**, *8* (38), 9870–9876.
- (32) Kim, H.; Walker, S. *Escherichia coli* transport in porous media: Influence of cell strain, solution chemistry, and temperature. *Colloids Surf., B* **2009**, *71* (1), 160–167.
- (33) van Merode, A. E. J.; Pothoven, D. C.; van der Mei, H. C.; Busscher, H. J.; Krom, B. P. Surface charge influences enterococcal prevalence in mixed-species biofilms. *J. Appl. Microbiol.* **2007**, *102* (5), 1254–1260.
- (34) Ojeda, J. J.; Romero-Gonzalez, M. E.; Bachmann, R. T.; Edyvean, R. G. J.; Banwart, S. A. Characterization of the cell surface and cell wall chemistry of drinking water bacteria by combining XPS, FTIR spectroscopy, modeling, and potentiometric titrations. *Langmuir* **2008**, *24* (8), 4032–4040.
- (35) Cunliffe, D.; Smart, C. A.; Alexander, C.; Vulfson, E. N. Bacterial adhesion at synthetic surfaces. *Appl. Environ. Microbiol.* **1999**, *65* (11), 4995–5002.
- (36) Cerca, N.; Pier, G. B.; Vilanova, M.; Oliveira, R.; Azeredo, J. Quantitative analysis of adhesion and biofilm formation on hydrophilic and hydrophobic surfaces of clinical isolates of *Staphylococcus epidermidis*. *Res. Microbiol.* **2005**, *156* (4), 506–514.
- (37) Pompilio, A.; Piccolomini, R.; Picciani, C.; D'Antonio, D.; Savini, V.; Di Bonaventura, G. Factors associated with adherence to and biofilm formation on polystyrene by *Stenotrophomonas maltophilia*: The role of cell surface hydrophobicity and motility. *FEMS Microbiol. Lett.* **2008**, *287* (1), 41–47.
- (38) Diaz, C.; Schilardi, P. L.; Dos Santos Claro, P. C.; Salvarezza, R. C.; Fernandez Lorenzo de Mele, M. A. Submicron trenches reduce the *Pseudomonas fluorescens* colonization rate on solid surfaces. *ACS Appl. Mater. Interfaces* **2009**, *1* (1), 136–143.
- (39) Hou, S.; Gu, H.; Smith, C.; Ren, D. Microtopographic patterns affect *Escherichia coli* biofilm formation on poly(dimethylsiloxane) surfaces. *Langmuir* **2011**, *27* (6), 2686–2691.
- (40) Meel, C.; Kouzel, N.; Oldewurtel, E. R.; Maier, B. Three-dimensional obstacles for bacterial surface motility. *Small* **2012**, *8* (4), 530–534.
- (41) Gibiansky, M. L.; Conrad, J. C.; Jin, F.; Gordon, V. D.; Motto, D. A.; Mathewson, M. A.; Stopka, W. G.; Zelasko, D. C.; Shrout, J. D.; Wong, G. C. L. Bacteria use type IV pili to walk upright and detach from surfaces. *Science* **2010**, *330* (6001), 197.
- (42) Jin, F.; Conrad, J. C.; Gibiansky, M. L.; Wong, G. C. L. Bacteria use type-IV pili to slingshot on surfaces. *Proc. Natl. Acad. Sci. U. S. A.* **2011**, *108* (31), 12617–12622.
- (43) Gibiansky, M. L.; Hu, W.; Dahmen, K. A.; Shi, W.; Wong, G. C. L. Earthquake-like dynamics in *Myxococcus xanthus* social motility. *Proc. Natl. Acad. Sci. U. S. A.* **2013**, *110* (6), 2330–2335.
- (44) Berg, H. C. *E. coli in Motion*; Springer: New York, 2004.
- (45) Walker, S. L.; Redman, J. A.; Elimelech, M. Influence of growth phase on bacterial deposition: Interaction mechanisms in packed-bed column and radial stagnation point flow systems. *Environ. Sci. Technol.* **2005**, *39* (17), 6405–6411.
- (46) Hunter, R. J. *Zeta Potential in Colloid Science*; Academic Press: New York, 1981.
- (47) Wu, S. Surface and interfacial tensions of polymer melts. II. Poly(methyl methacrylate), poly(*n*-butyl methacrylate), and polystyrene. *J. Phys. Chem.* **1970**, *74* (3), 632–638.
- (48) Shirley, D. A. High-resolution X-ray photoemission spectrum of the valence bands of gold. *Phys. Rev. B* **1972**, *5* (12), 4709.
- (49) Heydorn, A.; Ersboll, B.; Hentzer, M.; Parsek, M. R.; Givskov, M.; Molin, S. Experimental reproducibility in flow-chamber biofilms. *Microbiology* **2000**, *146*, 2409–2415.
- (50) Mohraz, A.; Solomon, M. J. Direct visualization of colloidal rod assembly by confocal microscopy. *Langmuir* **2005**, *21* (12), 5298–5306.
- (51) Hou, S.; Burton, E. A.; Simon, K. A.; Blodgett, D.; Luk, Y.-Y.; Ren, D. Inhibition of *Escherichia coli* biofilm formation by self-assembled monolayers of functional alkanethiols on gold. *Appl. Environ. Microbiol.* **2007**, *73* (13), 4300–4307.
- (52) Gu, H.; Hou, S.; Yongyat, C.; De Tore, S.; Ren, D. Patterned biofilm formation reveals a mechanism for structural heterogeneity in bacterial biofilms. *Langmuir* **2013**, *29* (35), 11145–11153.
- (53) Salerno, M. B.; Logan, B. E.; Velegol, D. Importance of molecular details in predicting bacterial adhesion to hydrophobic surfaces. *Langmuir* **2004**, *20* (24), 10625–10629.
- (54) Berg, H. C.; Turner, L. Torque generated by the flagellar motor of *Escherichia coli*. *Biophys. J.* **1993**, *65* (5), 2201–2216.
- (55) Neuman, K. C.; Chadd, E. H.; Liou, G.; Bergman, K.; Block, S. M. Characterization of photodamage to *Escherichia coli* in optical traps. *Biophys. J.* **1999**, *77* (5), 2856–2863.
- (56) Vigeant, M. A.-S.; Wagner, M.; Tamm, L. K.; Ford, R. M. Nanometer distances between swimming bacteria and surfaces measured by total internal reflection aqueous fluorescence microscopy. *Langmuir* **2001**, *17* (7), 2235–2242.

(57) Anderson, B. N.; Ding, A. M.; Nilsson, L. M.; Kusuma, K.; Tchesnokova, V.; Vogel, V.; Sokurenko, E. V.; Thomas, W. E. Weak rolling adhesion enhances bacterial surface colonization. *J. Bacteriol.* **2007**, *189* (5), 1794–1802.

(58) Gottenbos, B.; Grijpma, D.; Van Der Mei, H. C.; Feijen, J.; Busscher, H. J. Antimicrobial effects of positively charged surfaces on adhering Gram-positive and Gram-negative bacteria. *J. Antimicrobiol. Chemother.* **2001**, *48* (1), 7–13.

(59) Acres, R. G.; Ellis, A. V.; Alvino, J.; Lenahan, C. E.; Khodakov, D. A.; Metha, G. F.; Andersson, G. G. Molecular structure of 3-aminopropyltriethoxysilane layers formed on silanol-terminated silicon surfaces. *J. Phys. Chem. C* **2012**, *116* (10), 6289–6297.

(60) McClaine, J.; Ford, R. M. Characterizing the adhesion of motile and nonmotile *Escherichia coli* to a glass surface using a parallel-plate flow chamber. *Biotechnol. Bioeng.* **2002**, *78* (2), 179–189.

(61) Gomez-Suarez, C.; Pasma, J.; van der Borden, A.; Wingender, J.; Flemming, H.-C.; Busscher, H. J.; Van Der Mei, H. C. Influence of extracellular polymeric substances on deposition and redeposition of *Pseudomonas aeruginosa* to surfaces. *Microbiology* **2002**, *148*, 1161–1169.